MULTISCALE DYNAMIC DIFFUSION METHOD TO SOLVE ADVECTION-DIFFUSION PROBLEMS

Andrea M. P. Valli, **Lucia Catabriga**, **Isaac P. Santos**
avalli@inf.ufes.br, luciac@inf.ufes.br, isaacps@gmail.com
Universidade Federal do Espírito Santo
Av. Fernando Ferrari, 514, Goiabeiras, 29075-910, Vitória, ES, Brazil

Alvaro L. G. A. Coutinho
alvaro@nacad.ufrj.br
Programa de Engenharia Civil, COPPE, Universidade Federal do Rio de Janeiro
Caixa Postal 68501, 21941-972, Rio de Janeiro, RJ, Brazil

Regina C. Almeida
rcca@lncc.com
Laboratório Nacional de Computação Científica
Av. Getúlio Vargas, 333, Quitandinha, 25651-075, Petrópolis, RJ, Brazil

Abstract. *In this work we evaluate different characteristic subgrid parameters, such as the subgrid velocity field and the length scale at which the subgrid inertial effects take place, for a finite element formulation for advection-diffusion problems using a two-scale method denominated Dynamic Diffusion method (DD). To reduce the computational cost typical of two-scale methods, the subgrid scale space is defined using bubble functions whose degrees of freedom are locally eliminated in favor of the degrees of freedom that live on the resolved scales. This method leads to a nonlinear scheme which is solved by an iteration-lagging procedure that utilizes the bubble-enriched Galerkin solution as the correspondent initial approximation. Here we evaluate four different choices for the subgrid length scale used to define the amount of artificial diffusivity that should be added to the numerical model in the DD method. Numerical experiments were conducted to illustrate the behavior of the DD formulation for those different choices applied to advection-diffusion equations. Performance and accuracy comparisons are based on benchmark 2D problems.*

Keywords: *Multiscale Dynamic Diffusion, Finite Element, Advection-Diffusion Problems, Subgrid Length Scale*

1 INTRODUCTION

The problem we are interested in is the advection-diffusion equation in the case in which advection effects are dominant. It is well known that its numerical solution is still a challenge since the solutions typically carry interior and boundary layers, which are small subregions where the derivatives of the solution are very large. The basic difficulty is that the widths of these layers are usually significantly smaller than the mesh size and consequently they cannot be resolved properly (Donea & Huerta (2003)).

Considerable information contained in small scales and whose effects are not represented on the large ones leads to unwanted spurious (nonphysical) oscillations in the numerical solution. To overcome these difficulties, different methodologies have been developed in the literature. Various finite element stabilization strategies have been developed to enhance the stability and accuracy of the Galerkin discretization by adding linear perturbation terms containing mesh depending stabilizing parameters.

The success of these methodologies depends on a suitable design of the stabilization parameter (John & Knobloch (2007, 2008)). Since linear monotone methods can be at most first–order accurate and are usually not able to remove localized spurious oscillations for nonsmooth solutions, it is natural to add a nonlinear term to the linear formulation to enhance stability. Methods using this procedure are referred to as discontinuity capturing, as the Consistent Approximate Upwind Petrov-Galerkin (CAU) finite element method (Almeida & Galeão (1996)).

In the last years, stabilized methods have been reformulated in the context of the numerical multiscale formulation by enriching the piecewise linear functions with special local functions such as bubble functions (Hughes (1995); Brezzi et al. (1992)). Additional stabilization is provided by this enrichment via terms obtained by static condensation. The approximations of the fine scales emanating from the enrichments improve the resolved (coarse) scale solutions.

In this paper, we concentrate on the solution using the finite element method in the context of the numerical multiscale formulation (Coutinho et al. (2011)). We use the two scale method named Dynamic Diffusion method (DD) following the work presented in (Santos & Almeida (2007); Santos et al. (2012); Arruda et al. (2010)). The main idea of the method is to assume a two-level decomposition of the velocity field into the resolved (coarse) and unresolved (subgrid) scales, with respect to the grid scales. The subgrid velocity is designed to be the smallest one that is able to avoid kinetic energy accumulation associated with the coarse scales.

The DD method results in a free user-defined parameter method and its methodology outperforms some subgrid diffusion approaches for transport problems as well as some discontinuity capturing methods. The small scale space is defined using bubble functions whose degrees of freedom are condensed onto the resolved scale degrees of freedom. The methodology leads to a nonlinear scheme which is solved by an iteration-lagging procedure that utilizes the bubble-enriched Galerkin solution as the correspondent initial approximation. Here, we evaluate different ways to represent the amount of artificial diffusivity that should be added by the numerical model.

The remainder of this work is organized as follows. Section 2 briefly addresses the variational multiscale formulation. Numerical experiments are conducted in Section 3 to show the behavior of the proposed methodologies for a variety of benchmark transport problems. Section 4 concludes this paper.

2 THE VARIATIONAL MULTISCALE FORMULATION

This paper is devoted to the numerical solution of the scalar advection-diffusion equation

$$-\epsilon\,\Delta u + \boldsymbol{\beta}\cdot\boldsymbol{\nabla} u = f \qquad \text{in } \Omega; \tag{1}$$

$$u = g \qquad \text{on } \Gamma, \tag{2}$$

where $\Omega \subset \mathbb{R}^2$ is a bounded domain with a polygonal boundary Γ, ϵ is the constant diffusivity, $\boldsymbol{\beta}$ is a given velocity field satisfying the incompressibility condition $div\,\boldsymbol{\beta} = 0$, f is a given source/sink, and g represents the Dirichlet boundary condition. It is assumed that $\boldsymbol{\beta} \in W^{1,\infty}(\Omega)$, $g \in H^{1/2}(\Gamma)$ and $f \in L^2(\Omega)$.

In order to derive the multiscale formulation for Eq.(1) and Eq.(2), we have to introduce some notation. To reduce the computational cost typical of two-scale methods, the small scale space is defined using bubble functions whose degrees of freedom are condensed onto the resolved scale degrees of freedom. We consider a triangular partition $\mathcal{T}_H$ of the domain Ω into n_{el} elements, where: $\Omega = \bigcup_{e=1}^{n_{el}} \Omega_e$ and $\Omega_i \cap \Omega_j = \emptyset$, $i, j = 1, 2, \cdots, n_{el}$, $\quad i \neq j$. By denoting $\psi_B \in H_0^1(\Omega_e)$ as the bubble function defined in each element Ω_e, we define $V_B^{\Omega_e} = span(\psi_B)$. The discrete settings are then defined by introducing the following two spaces: $V_h = \{u_h \in H_0^1(\Omega) \mid u|_{\Omega_e} \in \mathbb{P}_1(\Omega_e),\ \forall \Omega_e \in \mathcal{T}_H,\ u|_\Gamma = g\}$ and $V_B = \oplus|_{\Omega_e} V_B^{\Omega_e}$ where $\mathbb{P}_1(\Omega_e)$ represents the set of first order polynomials in Ω_e. The bubble function used is a cubic polynomial function defined by

$\psi_B = 27 N_1^e(x,y) N_1^e(x,y) N_1^e(x,y)$, where N_j^e represents the local finite element function associated with the nodal point (coarse) j, $j = 1, 2, 3$ of element Ω_e. We introduce an additional discrete space V_E, such that the decomposition $V_E = V_h \oplus V_B$ holds, where V_h is the resolved (coarse) scale space whereas V_B is the subgrid (fine) scale space (Fig. 1).

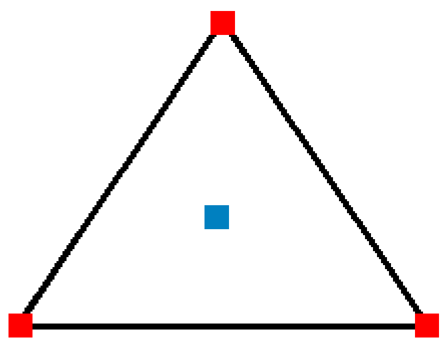

Figure 1. V_E **Representation.**

The Dynamic Diffusion method can be described as follows: find $u_E = u_h + u_B \in V_E$ with $u_h \in V_h$, $u_B \in V_B$ such that

$$A(u_E, w_E) \equiv B(u_E, w_E) + \sum_{e=1}^{nel} D(u_h; u_E, w_E) = (f, w_E) \quad \forall w_E \in V_E, \tag{3}$$

where $(\cdot,\cdot)$ is the $L^2(\Omega)$ inner product, $B(u,w) = \epsilon(\boldsymbol{\nabla} u, \boldsymbol{\nabla} w) + (\boldsymbol{\beta}\cdot\boldsymbol{\nabla} u, w)$, and the (local) nonlinear operator $D(.;.,.)$ is given by

$$D(u_h; u_E, w_E) = \int_{\Omega_e} \epsilon_k(u_h) \boldsymbol{\nabla} u_E \cdot \boldsymbol{\nabla} w_E \, d\Omega. \tag{4}$$

The coefficient $\epsilon_k(u_h)$ represents the amount of artificial diffusion added by the numerical model. Its design is based on the two-level decomposition of the velocity field into the resolved (coarse) and unresolved (subgrid) scales, with respect to the grid scales, as

$$\boldsymbol{\beta} = \boldsymbol{\beta}_h + \boldsymbol{\beta}_B. \tag{5}$$

The subgrid velocity field $\boldsymbol{\beta}_B$ is determined by requiring the minimum of the associated kinetic energy ($E_k = \frac{1}{2} |\boldsymbol{\beta}_B|^2$) for which the residual of the resolved scale solution (with $\boldsymbol{\beta}_h$) vanishes, inspired by the CAU method (Galeão & Carmo (1988)). Specifically, it is designed to be the smallest one that is able to avoid kinetic energy accumulation associated with the resolved (coarse) scale. The solution of this minimization problem yields a subgrid velocity field at each finite element in the form

$$\boldsymbol{\beta}_B = \frac{R(u_h)}{||\boldsymbol{\nabla} u_h||^2} \boldsymbol{\nabla} u_h \quad \text{if } ||\boldsymbol{\nabla} u_h|| \neq 0, \tag{6}$$

where $R(u_h) = -\epsilon \Delta u_h + \boldsymbol{\beta} \cdot \boldsymbol{\nabla} u_h - f$, and the subgrid velocity vanishes when $\boldsymbol{\nabla}\, u_h = \mathbf{0}$. Effectively, that is a projection of the coarse scale residual along the gradient of the resolved scale solution when $\boldsymbol{\nabla}\, u_h \neq \mathbf{0}$. Now, defining the subgrid length scale by $\hbar$, the amount of subgrid viscosity required to dissipate the kinetic energy E_k is defined as

$$\epsilon_k(u_h) = \frac{1}{2} \hbar ||\boldsymbol{\beta}_B|| \tag{7}$$

and the DD model term is given by

$$D(u_h; u_E, w_E) = \int_{\Omega_e} \epsilon_k(u_h) \boldsymbol{\nabla} u_E \cdot \boldsymbol{\nabla} w_E \, d\Omega \quad \text{if } ||\boldsymbol{\nabla} u_h|| \neq 0 \tag{8}$$

and $D(u_h; u_E, w_E) = 0$ otherwise. It is important to notice that it is a free user-defined parameter method since the artificial diffusion $\epsilon_k(u_h)$ is not a priori determined but is evaluated based on the resolved scale approximate solution u_h. However, the subgrid length scale must be defined a priori. Here, in the numerical examples, we use the following choices for the subgrid length scale $\hbar$:

(A1) $\hbar = \sqrt{A^e}$ where A^e is the area of the finite element Ω_e;

(A2) $\hbar = 2||\boldsymbol{\beta}_B||/||b||$, where $b = \boldsymbol{\beta}_B \cdot (\boldsymbol{x}_{,\epsilon_k})$ and the tensor $(\boldsymbol{x}_{,\epsilon_k})$ represents the Jacobian of the coordinate transformation (Brooks & Hughes (1982)). This choice implies that the the length scale takes into the account the direction of the subgrid velocity, decreasing the dependence of the solution with the mesh orientation;

(A3) $\hbar = t(\boldsymbol{\beta})/\|\boldsymbol{\beta}\|$ where $t(v) = \frac{1}{v} \max \{|\vec{AB} \cdot v|, |\vec{AC} \cdot v|, |\vec{BC} \cdot v|\}$ with A, B, C the vertices of the triangle (element) (Buscaglia & Dari (1997));

(A4) $\hbar = t(\boldsymbol{\beta}_B)/\|\boldsymbol{\beta}_B\|$.

Given the Eq. (3), (7) and (8), we design the method considering the following cases:

1. when $||\boldsymbol{\nabla}\, u_h|| = 0$, we have $||\boldsymbol{\beta}_B|| = 0$ so that $A(u_E, w_E) = B(u_E, w_E)$, recovering the Galerkin method enriched by the bubble functions locally. In this case, no extra stability term is needed;
2. when $||\boldsymbol{\nabla}\, u_h|| \neq 0$, we obtain the subgrid velocity field at each finite element (6), an extra dissipation mechanism given by (8) is added to the Galerkin formulation, which enhances the stability through the nonlinear operator.

The nonlinear formulation is solved using iteration-lagging scheme in which $\epsilon_k(u_h)$ (or $\boldsymbol{\beta}_B$) is delayed one iteration. The initial guess u_h^0 is built using the bubble-enriched Galerkin solution. To improve convergence, the following average rule to determine $\epsilon_k(u_h)$ is used in the experiments (Santos & Almeida (2007)):

$$\begin{aligned} \epsilon_k(u_h^i) &= \vartheta^{i+1}\hbar; \\ \vartheta^{i+1} &= \omega\hat{\vartheta}^{i+1} + (1-\omega)\vartheta^i, \text{ with } \omega \in [0,1] \text{ suitably chosen;} \\ \hat{\vartheta}^{i+1} &= \begin{cases} \frac{1}{2}\frac{|R(u_h^i)|}{||\boldsymbol{\nabla} u_h^i||}, & \text{if } ||\boldsymbol{\nabla} u_h^i|| > tol_{\epsilon_k}; \\ \\ 0, & \text{otherwise,} \end{cases} \end{aligned} \tag{9}$$

where the superscript i denotes the iterative step with $i = 0, 1, 2, \cdots$ until convergence. In the numerical experiments, we consider $tol_{\epsilon_k} = 10^{-10}$, $\omega = 0.5$ and $\hat{\vartheta}^0 = 0$. The nonlinear convergence is checked for the resolved scale degrees of freedom, under a given prescribed relative tolerance (tol_{nl}).

3 NUMERICAL RESULTS

In the experiments the domain Ω is discretized into N-by-N cells with two triangular elements in each cell, resulting in $(N+1)^2$ nodes and $2N^2$ elements. Our methodology is compared here with the bubble-enriched Galerkin (Galerkin+Bubble) solution and the Consistent Approximate Upwind Petrov-Galerkin (CAU) solution, using the formulation developed in (Almeida & Galeão (1996)) to prevent spurious oscillation generated by the dominance of the advection terms in the differential equations.

3.1 Convergence rates

In the first example, we numerically evaluate the convergence rates of the DD method for an advection-diffusion problem with a smooth solution, given by

$$u(x, y) = \sin(\pi x)\, \sin(\pi y) \quad \text{in } \Omega = (0, 1) \times (0, 1), \tag{10}$$

where the source term is chosen to satisfy Eq. (1), Dirichlet boundary conditions (2), $\epsilon = 10^{-6}$ and $\boldsymbol{\beta} = (1, 0)^T$. Figures 2(a) and 2(b) show the linear approximation of the solution errors associated with the DD and CAU methods, measured in the $L^2(\Omega)$ and $H^1(\Omega)$ norms respectively. The error is plotted against mesh size on a log-log scale. The approximate solutions are computed for a sequence of five uniform meshes with 32-by-32, 40-by-40, 48-by-48, 60-by-60 and 80-by-80 cells, and we consider $tol_{nl} = 0.01$. Optimal convergence rates are obtained for both methods and different choices for $\hbar$, (A1)-(A4). The convergence rates are similar to the SUPG (Streamline-Upwind/Petrov-Galerkin) stabilization technique (Brooks & Hughes (1982)). For example, the respective approximate slopes of 1.01 and 1.87 for DD(A1) method indicate global rates of convergence. The errors of the DD(A1)-(A4) methods are alike and the CAU method yields highest errors. We may also notice that the DD(A2) and CAU methods present slightly higher convergence rates but they lead to the highest errors. DD(A1) presents the simple choice for $\hbar$ and it produces the smallest errors for this problem.

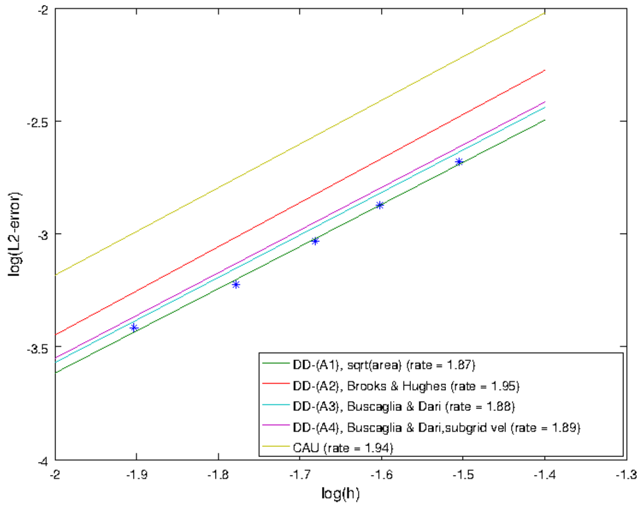

(a) $L^2(\Omega)$ norm

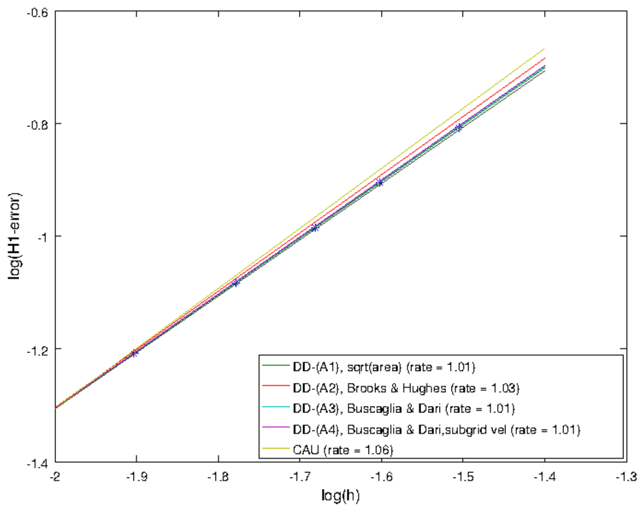

(b) $H^1(\Omega)$ norm

Figure 2. Convergence rates for the regular solution $u(x,y) = \mathbf{sin}(\pi x)\mathbf{sin}(\pi y) \in \Omega$.

3.2 Advection in a rotating flow field

The second experiment is an advection dominated problem presented in (Brooks & Hughes (1982)), where the flow is a rigid rotation about the center of a unit square domain, $\Omega = [-0.5, 0.5] \times [-0.5, 0.5]$. Figure 3 shows the boundary conditions of the problem. The solution u is set to zero on the external boundary of the square, and u is prescribed to be a sine hill on the internal 'boundary' $OA = \{x = 0; -0.5 \leq y \leq 0\}$, $u = -sin(2\pi\, y)$. The velocity field is $\boldsymbol{\beta} = (-y, x)$, $f = 0$ and $\epsilon = 10^{-8}$. The exact solution is essentially a pure advection of the OA boundary condition along the circular streamlines.

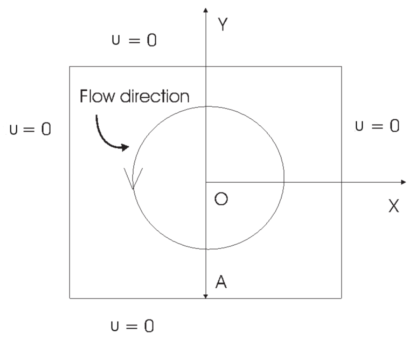

Figure 3. Advection in a rotating flow field: problem statement.

Figure 4 shows the elevation of u_h using Galerkin+Bubble, CAU and DD(A1)-(A4) methods for a mesh with 40-by-40 cells and $tol_{nl} = 0.1$. All methods (with the exception of Galerkin+Bubble scheme) introduce a non-physical dissipation at the internal border. In this example, the approximation given by the Galerkin+Bubble method provides a very good solution when compared with the exact solution, while all the other methods present an excessive amount of dissipation at the inner border. This solution is used as the initial solution for DD(A1)-(A4) methods and we can observe in Fig. 4 that DD(A1) produces the best numerical solution among them. The numerical dissipation at the internal border can be better observed in the profile depicted in Fig. 5 for Galerkin+Bubble, CAU and DD(A1) methods.

3.3 Variable flow-field

The third example has a discontinuity in the inlet profile introducing a thin boundary layer at the right boundary (Shih & Elman (2000)). The problem is defined in the rectangular region $\Omega = (-1, 1) \times (-1, 1)$, with velocity field $\boldsymbol{\beta} = (2y(1-x^2), -2x(1-y^2))$, $f = 0$ and $\epsilon = 10^{-6}$. Dirichlet boundary conditions specified in the inflow boundary, $\{(x, 0)| -1 \leq x \leq 0\}$, represent a temperature which is advected in a circular flow to the outflow boundary, $\{(x, 0)|\; 0 < x < 1\}$, where natural boundary conditions $\frac{\partial u(x,0)}{\partial n} = 0$ are assigned. The inlet boundary condition is

$$u(x, 0) = \begin{cases} 0, & -1 \leq x < -0.5 \\ 1, & -0.5 \leq x \leq 0 \end{cases}$$

and Dirichlet boundary conditions are prescribed on: $u(-1, y) = 0$ and $u(1, y) = 1$ for $0 < y < 1$; and $u(x, 1) = 0$ for $-1 < x < 1$. Representative pictures of the three-dimensional structure of the numerical solutions obtained by Galerkin+Bubble, CAU and DD(A1)-(A4) methods tested, for a mesh with 80-by-40 cells and $tol_{nl} = 0.01$, are shown in Fig. 6. We can observe in the pictures that all methods yield solutions with undershoots, oscillations and smearing. However, DD(A2) yields the qualitatively best solution with no overshoots and considerably less oscillations. The CAU method also produces a good solution, but it does not eliminate overshoots. In this example, DD(A1) leads to excessive overshoots, undershoots, and some oscillations near internal layers.

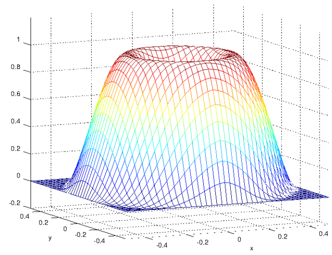

(a) Galerkin+Bubble

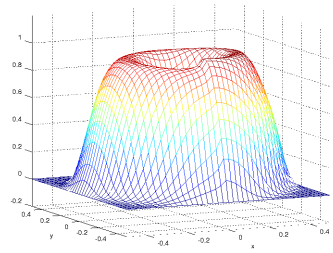

(b) CAU

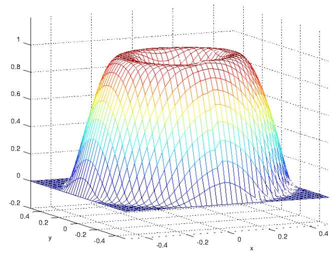

(c) DD(A1)

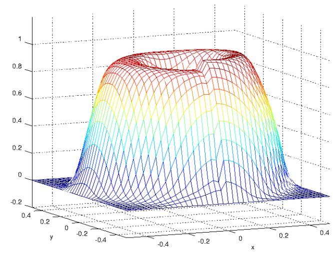

(d) DD(A2)

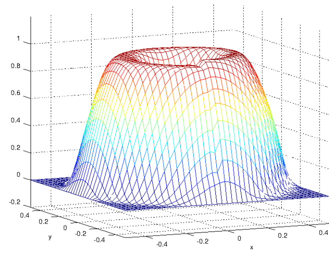

(e) DD(A3)

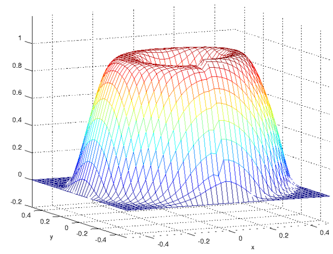

(f) DD(A4)

Figure 4. Advection in a rotating flow field: elevation of u_h.

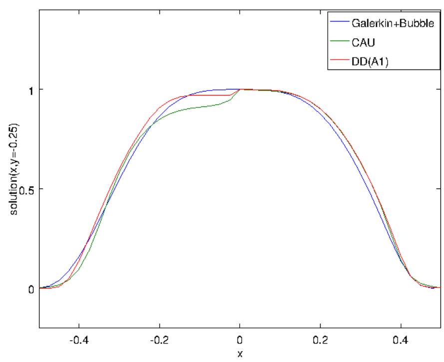

Figure 5. Advection in a rotating flow field: Galerkin+Bubble, CAU and DD(A1) solutions for $y = -0.25$.

3.4 Internal and external layers

This fourth example deals with a singular perturbed case yielding a solution with internal and external layers. Consider the transport problem defined in the rectangular region $\Omega = (0, 1) \times (0, 1)$, with velocity field $\boldsymbol{\beta} = (0.5, 1)$, $f = 0$ and $\epsilon = 10^{-6}$. The Dirichlet boundary

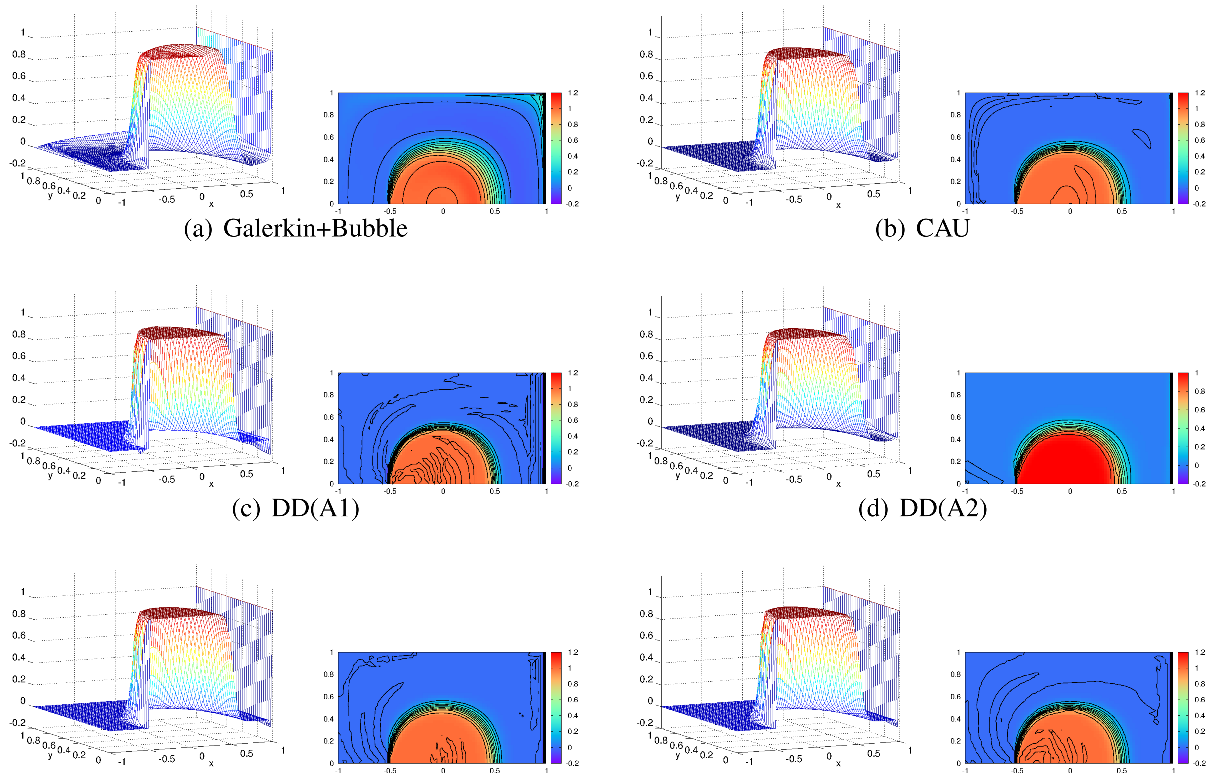

(a) Galerkin+Bubble (b) CAU

(c) DD(A1) (d) DD(A2)

(e) DD(A3) (f) DD(A4)

Figure 6. Variable flow-field problem: elevation of u_h.

conditions are

$$u(x,y) = \begin{cases} 1, & 0.3 < x \leq 1,\ y = 0; \\ 0, & \text{otherwise.} \end{cases}$$

Figure 7 shows the approximate solutions obtained by Galerkin+Bubble, CAU and DD(A1)-(A4) for a mesh with 40-by-40 cells and $tol_{nl} = 0.05$. The solutions possess an interior layer in the direction of the advection starting at $(0.3, 0)$ and an exponential external layer at the outflow, which comprises the sides $x = 1$ and $y = 1$ of the boundary. The approximate solutions obtained by CAU and DD(A2)-(A4) are very alike, but the results obtained with Galerkin+Bubble and DD(A1) are not free of spurious oscillations and smearing. Figure 8 shows the comparison between CAU and DD(A2)-(A4) solutions at $y = 0.5$ and $x = 0.9$. We can observe in this example that DD(A3) and DD(A4) approaches produce the best solutions.

3.5 Two internal layers

The last example possesses two interior layers and was first considered by (John & Knobloch (2008)) an exponential external layer. We consider the advection-diffusion equation with velocity field $\boldsymbol{\beta} = (1, 0)$, $\epsilon = 10^{-8}$, $\Omega = (0,1) \times (0,1)$ and

$$f(x,y) = \begin{cases} 16(1-2x), & (x,y) \in [0.25, 0.75] \times [0.25, 0.75]; \\ 0, & \text{otherwise.} \end{cases}$$

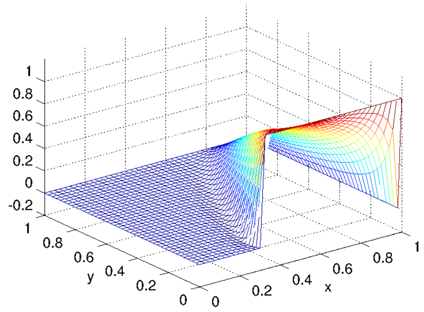

(a) Galerkin+Bubble

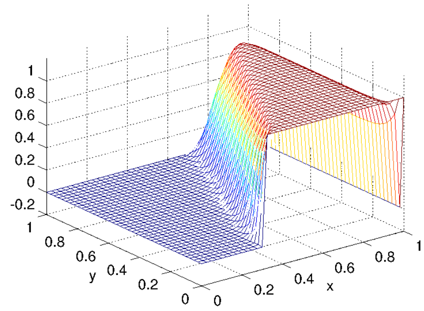

(b) CAU

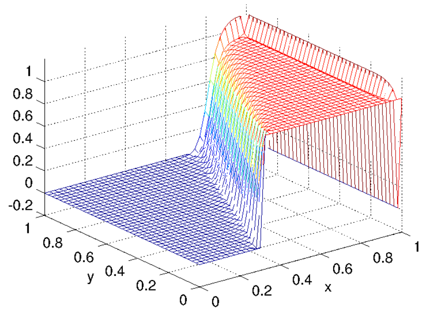

(c) DD(A1)

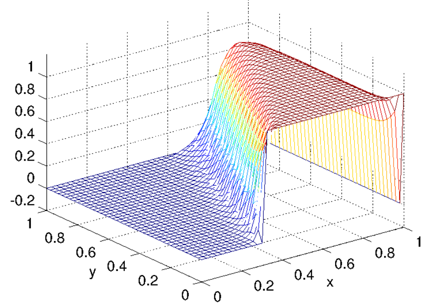

(d) DD(A2)

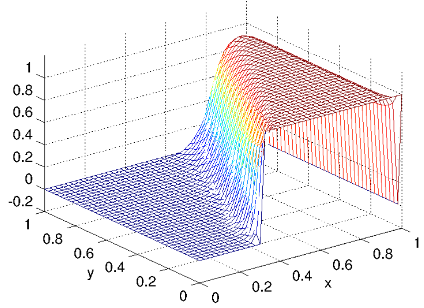

(e) DD(A3)

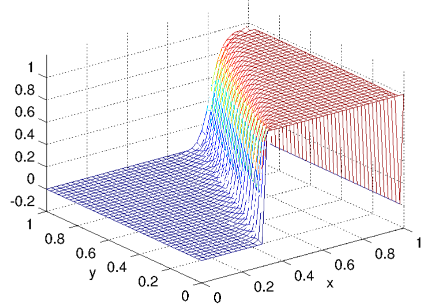

(f) DD(A4)

Figure 7. Advective-diffusive problem: internal and external layers.

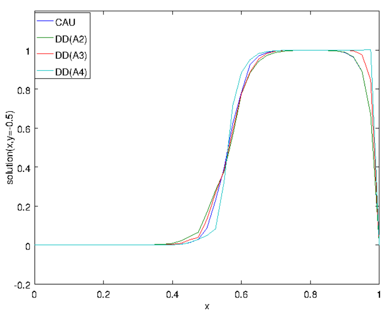

(a) $y = 0.5$

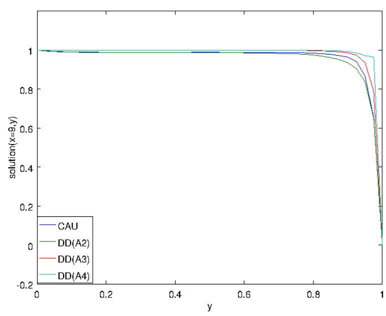

(b) $x = 0.9$

Figure 8. Internal and external problem: solutions at $y = 0.5$ and $x = 0.9$.

Homogeneous boundary conditions are considered in Ω, $g = 0$. The solution is very close to the quadratic function $u(x, y) = (4x - 1)(3 - 4x)$ in $(0.25, 0.75) \times (0.25, 0.75)$ and has interior layers at $(0.25, 0.75) \times 0.25$ and $(0.25, 0.75) \times 0.75$, see Fig. 9(a). The approximate solutions for all the methods are calculated using a mesh with 40-by-40 cells and $tol_{nl} = 0.1$. Note (Fig. 9(a)) that all solutions present undershoots and overshoots and they are also inaccurate in the region $(0.75, 1) \times (0, 1)$. The overshoots present in the Galerkin+Bubble solution are significantly small when compared with the other solutions. DD methods do not obtain a qualitatively correct approximation of the solution to this problem for $tol_{\epsilon_k} = 10^{-10}$. However, the solutions for DD(A1), DD(A3) and DD(A4) can be improved if we consider $tol_{\epsilon_k} = 10^{-3}$, as we can see in Fig. 10.

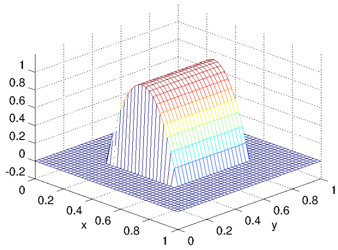

(a) Solution u

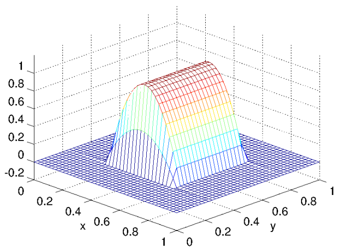

(b) Galerkin+Bubble

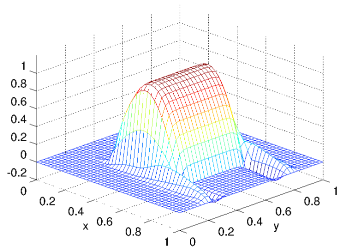

(c) CAU

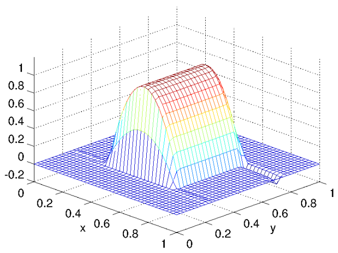

(d) DD(A1)

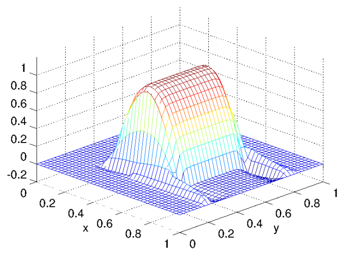

(e) DD(A2)

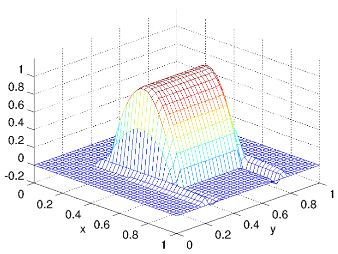

(f) DD(A3)

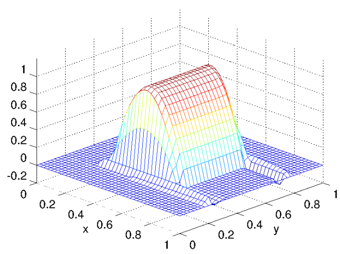

(g) DD(A4)

Figure 9. Two internal layers problem solutions for $tol_{\epsilon_k} = 10^{-10}$.

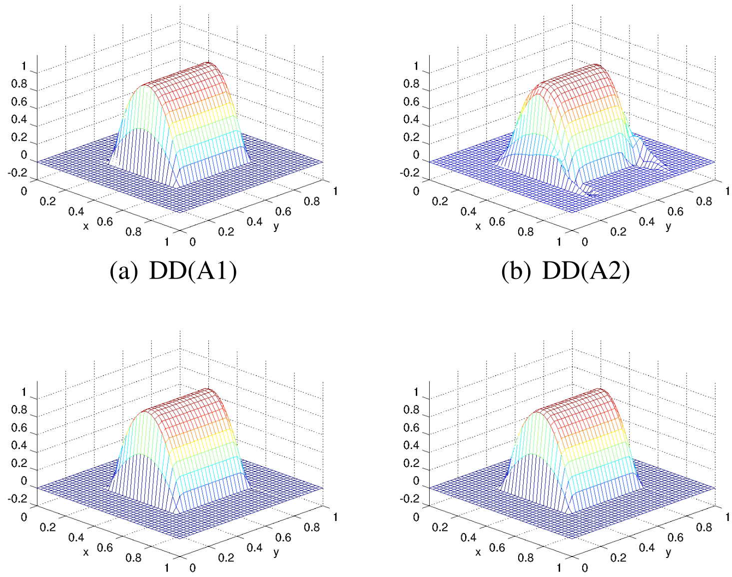

(a) DD(A1) (b) DD(A2)

(c) DD(A3) (d) DD(A4)

Figure 10. Two internal layers problem solutions for $tol_{\epsilon_k} = 10^{-3}$.

4 Conclusions

In this paper, we evaluate four different choices for the subgrid length scale used to define the amount of artificial diffusivity that should be added by the numerical model in the two-scale Dynamic Diffusion (DD) method. The choices involve calculations of the element area (A1), the subgrid velocity field together with the Jacobian of the coordinate transformation (A2), the vertices of the triangle with the convection field (A3), and the vertices of the triangle with the subgrid field (A4). We evaluate the performance of the methodologies for four benchmark 2D problems, and we numerically evaluate the convergence rates of the DD method for an advection-diffusion problem with a smooth solution. We obtain global rates of convergence for all the approaches similar to the SUPG stabilization technique, i.e. approximate slopes around 1 and 2 measured in the $L^2(\Omega)$ and $H^1(\Omega)$ norms respectively. DD(A1) presents the simple choice for the subgrid length scale and it produces the smallest errors for the problem with known solution. This method also produces the best solutions for the advection in a rotating flow field problem and the internal and external layers problem. However, DD(A1) does lead to unwanted spurious oscillations in the numerical solution of the other problems. DD(A2) is the best choice for the variable flow-field problem, and produces good solutions for almost all applications presented here (with the exception of the two interior layers problem). DD(A3) and DD(A4) produce good solutions for all problems, and DD(A4) is the best choice for the internal and external layers problem. Hence, both DD(A3) and DD(A4) can be faily choices for the subgrid length scale. Future experiments involve the study of different indicators of the quality/accuracy of the resolved scale solution in order to better regulate the amount of artificial diffusivity that should be added by the numerical model, such as the size of the gradient of the subscale solution at each element.

ACKNOWLEDGEMENTS

This work has been supported in part by CNPq, CAPES, FAPERJ and FAPES.

REFERENCES

Almeida, R. & Galeão, A., 1996. An adaptive Petrov-Galerkin formulations for the compressible Euler and Navier-Stokes equations, *Computer Methods in Applied Mechanics and Engineering* 129, 157–176.

Arruda, N., Almeida, R. & do Carmo, E., 2010. Dynamic diffusion formulation for advection dominated transport problems, *Mecánica Computacional* 29, 2011–2025.

Brezzi, F., Masud, A., Franca, L., Mallet, M. & Rogé, G., 1992. A relationship between stabilized finite element methods and the Galerkin method with bubble functions, *Computer Methods in Applied Mechanics and Engineering* 96, 117–129.

Brooks, A. & Hughes, T., 1982. Streamline upwind/Petrov-Galerkin formulations for convection dominated flows with particular emphasis on the incompressible Navier-Stokes equations, *Computer Methods in Applied Mechanics and Engineering* 32, 199–259.

Buscaglia, G. & Dari, E., 1997. Anisotropic mesh optimization and its application in adaptivity, *International Journal for Numerical Methods in Engineering* 40(22), 4119–4136.

Coutinho, A. L. G. A., Franca, L. & Valentin, F., 2011. Numerical multiscale methods, *International Journal for Numerical Methods in Fluids* 70, 403–419.

Donea, J. & Huerta, A., 2003. *Finite Element Methods for Flow Problems*, John Wiley and Sons Ltd.

Galeão, A. & Carmo, E. D., 1988. A consistent approximate speed-up upwind Petrov-Galerkin method for convection-dominated, *Comp. Meth. Appl. Mech. Eng.* 10, 83–95.

Hughes, T., 1995. Multiscale phenomena: Green's functions, the Dirichlet-to-Neumann formulation, subgrid scale models, bubbles, and the origins of stabilized methods, *Computer Methods in Applied Mechanics and Engineering* 127, 387–401.

John, V. & Knobloch, P., 2007. On spurious oscillations at layers diminishing (SOLD) methods for convection-diffusion equations: Part I - a review, *Computer Methods in Applied Mechanics and Engineering* 196(17-20), 2197–2215.

John, V. & Knobloch, P., 2008. On spurious oscillations at layers diminishing (SOLD) methods for convection-diffusion equations: Part II - analysis for P1 and Q1 finite elements, *Computer Methods in Applied Mechanics and Engineering* 197(21-24), 1997–2014.

Santos, I. P. & Almeida, R. C., 2007. A nonlinear subgrid method for advection-diffusion problems, *Computer Methods in Applied Mechanics and Engineering* 196, 4771–4778.

Santos, I. P., Almeida, R. C. & Malta, S., 2012. Numerical analysis of the nonlinear subgrid scale method, *Computational & Applied Mathematics* 31, 473–503.

Shih, Y. & Elman, H., 2000. Iterative methods for stabilized discrete convection–diffusion problems, *IMA Journal of Numerical Analysis* 20, 333–358.